

QVis: A Visual Analytics Tool for Exploring Noise and Errors in Quantum Computing Systems

Chad A. Steed, Junghoon Chae, Samudra Dasgupta, Travis S. Humble

Oak Ridge National Laboratory, Oak Ridge, USA

{steedca, chaej, dasguptas, humblets}@ornl.gov

Abstract—We present the preliminary design and results of *QVis*, a visual analytics tool for exploring quantum device performance data. *QVis* helps uncover temporal and multivariate variations in noise properties of quantum devices. We describe the implementations of these methods as well as applications to the analysis of a 127-qubit data set derived from the IBM washington processor over a 16-month period. Both human-interactive and semi-automated analytic methods are included to address requirements for visual exploration, thresholding, and clustering techniques. Our application of *QVis* to real-world scenarios demonstrates the ability to reveal noteworthy patterns in the behavior of the critical characterization metrics.

Index Terms—quantum computing, visual analytics, system reliability, clustering, temporal analysis

I. INTRODUCTION

Quantum computing offers remarkable methods for processing information, and the development of increasingly sophisticated quantum devices is vital for experimental demonstrations. Current devices, however, suffer from significant noise, including decoherence (T_2), that results in high error rates during computations. For example, Fig. 1 illustrates the probability distribution of the T_2 time for qubit 4 (Q4) of the transmon device named washington, based on daily data from IBM’s published characterizations from 1-Jan-2022 to 30-Apr-2023. The T_2 metric quantifies the duration before a quantum superposition state transitions into a classical state. In the quest to improve quantum devices and reduce such errors, understanding the sources of noise is essential.

As the complexity of quantum device architectures increases, it becomes more difficult to reason about noise and its impact on device performance [1], [2]. These evolving conditions only exacerbate temporal and multivariate analysis of performance data from quantum systems. To make sense of this data and uncover insights about noisy quantum device behaviors, researchers need more flexible analysis tools that enable exploration of real-world performance data.

This research used computing resources of the Oak Ridge Leadership Computing Facility, which is a DOE Office of Science User Facility supported under Contract DE-AC05-00OR22725. The manuscript is authored by UT-Battelle, LLC under Contract No. DE-AC05-00OR22725 with the U.S. Department of Energy. The U.S. Government retains for itself, and others acting on its behalf, a paid-up nonexclusive, irrevocable worldwide license in said article to reproduce, prepare derivative works, distribute copies to the public, and perform publicly and display publicly, by or on behalf of the Government. The Department of Energy will provide public access to these results of federally sponsored research in accordance with the DOE Public Access Plan. <http://energy.gov/downloads/doe-public-access-plan>.

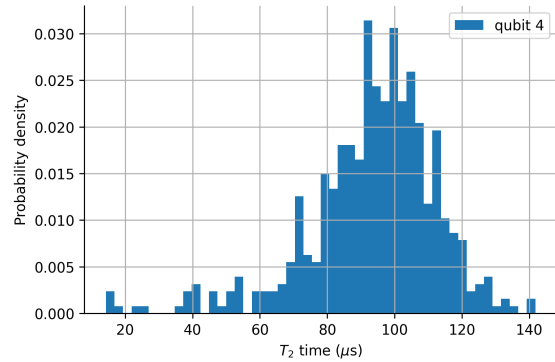


Fig. 1. The distribution of T_2 times observed for qubit 4 of the IBM transmon device washington for the period 1-Jan-2022 to 30-Apr-2023. The distribution of T_2 underlies variations in system behavior and fluctuations in computational errors that can be revealed through visual analytics.

In this paper, we address the challenge of reasoning about noise and error in quantum computing devices through the development of a visual analytics tool called *QVis*. *QVis* and the associated analytical methods we use for extracting temporal patterns are designed to enable human-directed analysis of performance data with guidance from semi-automated computational analytics. The tool is implemented as an interactive, web-based application with data visualizations that are implemented using the Data-Driven Documents (D3) JavaScript visualization library [3]. *QVis* is undergoing active development and is not yet available online, but we anticipate a public release date in the near future.

Our contribution presents the main features of the initial version of *QVis* and demonstrations of its utility by analyzing the temporal and statistical trends from quantum computing performance data. Since we are in the early stages of developing *QVis*, we also describe several anticipated extensions.

II. METHODS

A. Quantum System Performance Data

The data set analyzed in this paper was derived from a subset of the washington device characterization data collected during a 16-month period starting on 1-Jan-2022 and ending on 30-Apr-2023 [4]. The data set includes characterization metrics including state preparation and measurement (SPAM) error rate, gate error rate, gate duration, decay time (T_1) and decoherence (T_2) time. For demonstration of our analysis using *QVis* in this paper, we use the daily T_1 and T_2 characterization data. These metrics quantify the performance of

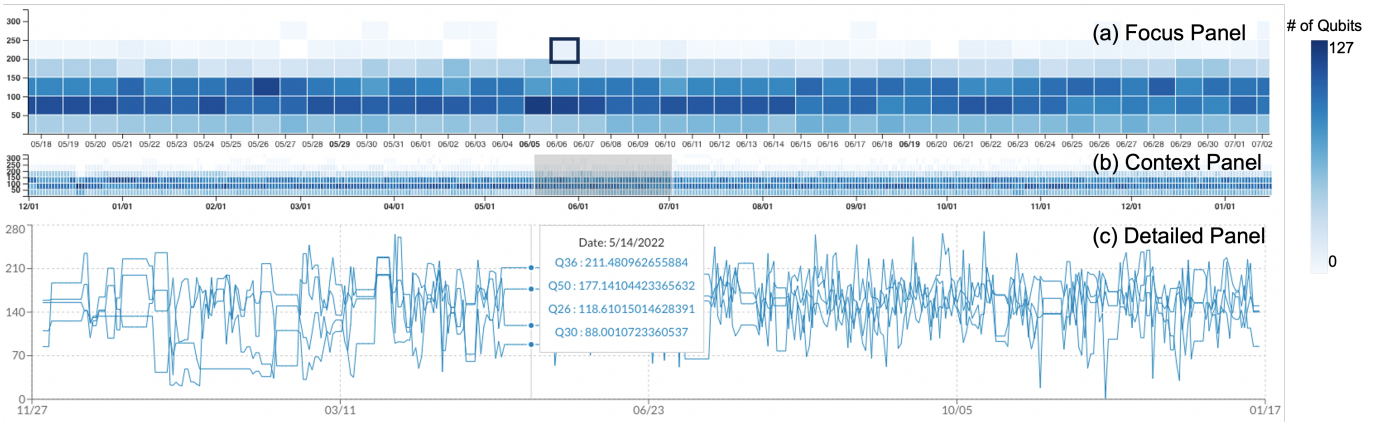


Fig. 2. *QVis* features three linked temporal visualizations: (a) focus view, (b) context view, and (c) detailed view. Panels (a) and (b) work together as a focus+context visualization using a binned representation of the current device metric. The bottom detailed panel (c) displays high fidelity line charts for qubits of interest. In this figure, values for T_2 metric are shown.

the register to store quantum information with higher values being more favorable.

B. Multiple-scale Temporal Visualization Methods

As shown in Fig. 2, *QVis* features a set of three interactive visualization panels for exploring temporal variability in quantum device data. In each visualization panel of the figure, the T_2 metric is displayed with the collection time mapped to the x -axis and the metric value to the y -axis. It is important to note that although we show only T_2 in the figure, the user can choose to view any of the available metrics in these panels.

The top two panels (see Figs. 2(a) and (b)) are linked together to provide a binned, focus+context visualization of high level trends for the qubits of interest (all qubits are included in the visualization shown in Fig. 2). These two panels show that T_2 parameters typically lie in the range of 50-100 μs but they fluctuate substantially in the remainder. The detailed panel (c) shows the raw time series of T_2 values from a subset of 4 qubits that are selected in the focus panel (Fig. 2(a)). These visualization panels and their interactive mechanisms are described in further detail in the remainder of this section.

1) *Focus+context Heatmaps*: The focus+context visualization approach is often used when analyzing temporal information because it allows users to see a smaller time range (the focus) and a wider time range (the context) simultaneously. The focus+context visualization panels in Fig. 2 show the data for the selected time range of interest in the focus panel while also showing the focus time range within the context of the overall data set in the lower context panel.

A time range of interest may be magnified by dragging a selection in the context view, shown as the gray rectangular region in Fig. 2(b). This action forces the focus view to redraw using the selected time range. The user can also fine tune the focus range selection by dragging either the start or end limit or by panning the entire time range selection. Here, the daily granularity of the data sets the minimum range. These interactions allow users to flexibly navigate to and

investigate various time ranges of interest at different scales while preserving contextual awareness of the whole.

The focus+context panels display aggregated representations of the raw metric data to avoid over-plotting and clutter issues that are often associated with displaying many time series records in a single plot. The aggregated view is constructed by partitioning the visible portion of the data into two-dimensional bins in both the y - and x -axis dimensions. In Fig. 2, presentation of the T_2 data yields insights into how coherence changes over the selected time range. The user can use menu components to adjust the bin size to refine the analysis. After the bin size is set, daily time series records for each qubit are processed and assigned to the appropriate bins based on the time and metric values. When the binning process is complete, each bin contains a list of associated qubits. The bins are visualized in the focus+context panels as color-filled heatmaps using the color scale shown on the right side of Fig. 2. The color scale indicates the number of qubits associated with each bin, with darker blues indicating a larger number of qubits.

Although the binned representation sacrifices the display of individual qubit values to maximize legibility, the contextual display preserves connections to the full data set and reveals broader temporal patterns. In addition, users can hover over a bin to access statistical summaries (e.g., the number of qubits, median value) in the form of a textual tooltip. A menu interface (not shown in Fig. 2) allows the user to specify the metric and specific qubits to generate customized views.

2) *Detailed Line Charts*: To access detailed time series information, the user can click on a bin in the top focus panel. This action causes the detailed visualization panel (see Fig. 2(c)) to show the time series information for qubits associated with the selected bin(s) as line graphs. In Fig. 2, the user has clicked on the bin with a black outline in the focus view, which resulted in drawing four qubit-specific line graphs in the detailed visualization panel. Each line corresponds to one of the four selected qubits (Q26, Q30, Q36, and Q50). As the user hovers over the detailed time series plot, a textual tooltip appears showing the numerical values for each

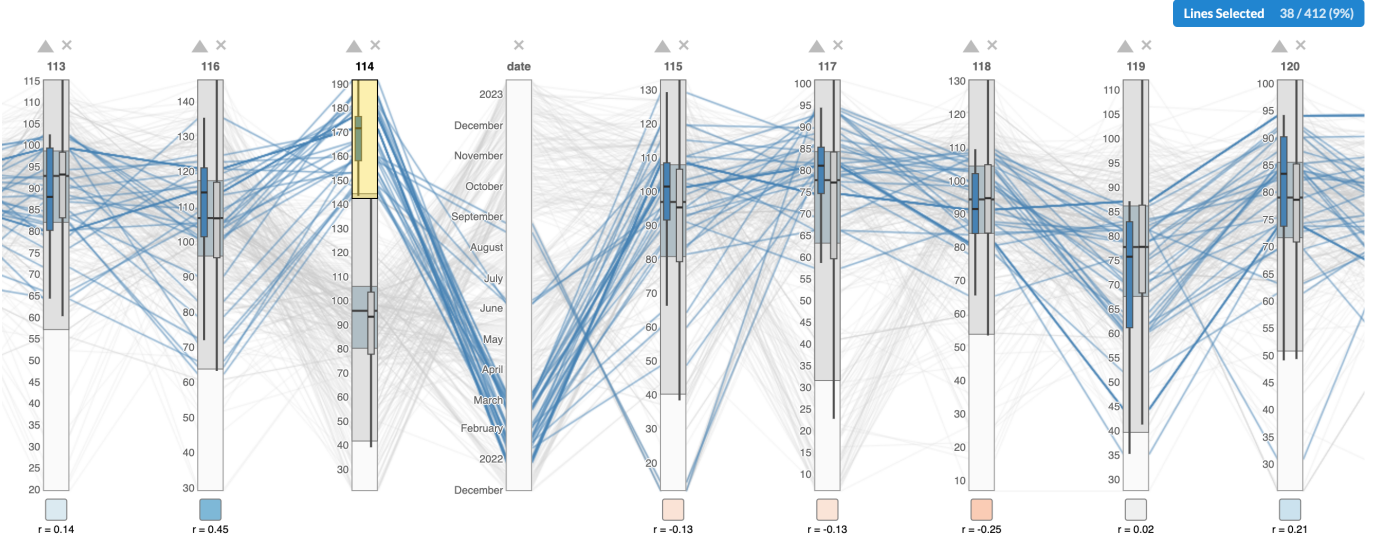


Fig. 3. Parallel coordinates plot of the T_1 metric where each vertical axis represents a qubit. The polylines represent individual daily values for all qubits. The statistical box plots show the high-level comparisons of the qubits. A selection on the upper range of Q114 highlights the associated days on the other qubit axes and the corresponding T_1 values.

line/qubit at a point in time.

Paired with the focus+context views, the detailed visualizations and dynamic hover queries provide a multiple-scale representation of the quantum device data. This approach follows the InfoVis Mantra design strategy, which suggests that visual analysis interfaces are most efficient when they provide overviews, zooming and filtering capabilities, and detailed information on demand [5].

C. Multivariate Visualizations

The multivariate nature of quantum device performance data is both an inherent complexity and opportunity to mine for correlations and trends. Using an extended variant of the parallel coordinates plot, we investigate trends and correlations between different qubit-specific metrics. As shown in Fig. 3, the parallel coordinates method we use augments the axis representations of the classic algorithm [6] with statistical summary information, namely box plots and correlation indicators. For more information about these parallel coordinate extensions the reader is directed to the paper on CrossVis [7].

In Fig. 3, each vertical axis in the parallel coordinate plot represents a qubit, except for the date axis that represents days of the year. Only a few qubits are shown in this figure, but all the qubits in the data set are accessible by scrolling to the left or right in the view. Each line represents a particular day. Where the lines intersect with the qubit axes represent the qubit's T_1 metric value on the day associated with the line. Although we are focused on the T_1 metric in this section, it is important to note that the user can select and analyze any of the device metrics through the application interface.

Fig. 3 also has a range selection set on the Q114 axis (see the yellow rectangular range at the top of the axis labeled 114). Because of this user-defined selection all lines that represent days with highest values of T_1 on Q114 are colored blue in the plot. The other unselected lines are colored a semi-transparent

gray that blends into the background. This selection shows that most of the high values for Q114 occurred between January and mid-March 2022, except for a few values in June and August of 2022. Such information could lead researchers to delve deeper into what caused these values and how changes beyond mid-March 2022 caused T_1 values to drop for Q114.

Fig. 3 also shows that the range of T_1 values for Q114 has a significantly higher upper limit than the other qubits in this data set. The upper limit is around $190 \mu\text{s}$ while the highest among the other qubits is at most about $150 \mu\text{s}$ (with the average being about $110 \mu\text{s}$). This observation provides further motivation for additional investigations into the behavior of Q114 and those that may be correlated with it, such as Q116 which has the highest correlation ($r = 0.45$) based on the selected range of lines/days in Fig. 3.

D. Temporal Clustering Analytics

In addition to interactive capabilities, the vision for *QVis* includes automated analytical methods that guide the user to potentially significant insights. *QVis*'s initial analytical offering focuses on a temporal clustering method. By clustering key quantum hardware metrics in time, the system supports understanding behaviors of the computing devices, extracting significant patterns, and identifying outliers.

We utilize a k-means clustering algorithm for time series data [8]. The clustering method is applied to each quantum computing metric in the data set. The metric's Euclidean distance is used where the distance between the i th point of one series and i th point of another is computed. Despite some limitations, such as being invariant to time shift, this approach supports grouping the time series data into daily behaviors (e.g., average value of each date). Additionally, the time series records for each qubit are of equal lengths, meaning we can avoid using Dynamic Time Warping (DTW) [9], which is a similarity measure for variable length time series

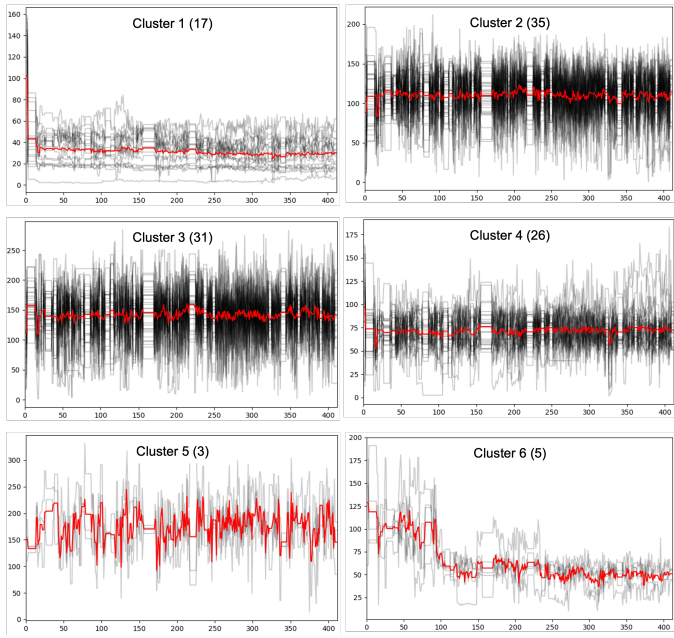


Fig. 4. This figure shows the K-means clustering results for T_2 metric in our sample quantum performance data set. Each individual plot represents a cluster with individual qubit profiles shown in black and the barycenter trends shown in red.

that would result in significant additional computation. The k-means clustering algorithm constructs clusters of data by splitting samples into k groups and minimizing the sum of squares in each cluster. Through trial and error, we decided to use 6 for the k parameter by default, but this parameter can be changed depending on the user's analytics objectives.

Fig. 4 shows the clustering results for T_2 metric data. Each subplot represents a cluster, where the x -axis is mapped to time and y -axis is mapped to the T_2 value. The semi-transparent black lines show the individual instances in the cluster and the red lines show each cluster's barycenter. The barycenter is the arithmetic mean for each individual point in time where the summed Euclidean distance is minimized for each of them. The number in the title of each plot in Fig. 4 shows the cluster size, or number of instances.

The barycenter of cluster 1 initially peaks, and then drops to about $30 \mu\text{s}$ where it remains. This pattern differs significantly from that of clusters 2, 3, and 4, which are larger overall and have more variance than cluster 1. However, the dominant values of the barycenters for 2, 3, and 4 are different from one another. For clusters 2, 3, and 4 the barycenter values are $110 \mu\text{s}$, $140 \mu\text{s}$, and $75 \mu\text{s}$, respectively. The sizes of clusters 5 and 6 are much smaller than the others, which indicates that these are outliers.

III. CONCLUSIONS

QVis and the supplemental analytical methods presented in this paper demonstrate a new capability to explore how noise and errors manifest in quantum computing devices. Our demonstration has used the daily T_1 and T_2 data characterizing the IBM Washington transmon device [4], but *QVis* is capable of analyzing other performance data on much smaller temporal

scales. The tool is already designed to analyze one- and two-qubit gate errors as well as asymmetric readout error. In addition to human-centered visualization techniques, we have demonstrated the application of temporal clustering metrics to identify multiple subsets of qubits that demonstrate common behaviors in the T_2 metric.

Quantum computing experts find *QVis*, even in its initial offering, to be a promising tool for informing future device performance studies and revealing insights into processor conditions that support reliable behavior. Future work will extend the temporal and multivariate analysis techniques and incorporate topological analytics. These efforts will also include the development of automated methods that reveal correlations and connections across performance metrics. Ultimately, we envision a tightly-coupled visual analytics system that is publicly accessible on the Internet and can dynamically pull performance metrics for multiple quantum computing devices to enable monitoring and benchmarking system performance. These tools are an important advance in understanding the stability and reliability of noisy quantum computing devices.

ACKNOWLEDGMENT

This research was supported by the US Department of Energy, Office of Science Early Career Research Program. This research used resources of the Oak Ridge Leadership Computing Facility, which is a DOE Office of Science User Facility supported under Contract DE-AC05-00OR22725.

REFERENCES

- [1] M. N. Lilly and T. S. Humble, "Modeling noisy quantum circuits using experimental characterization," *arXiv preprint arXiv:2001.08653*, 2020.
- [2] P. C. Lotshaw, T. Nguyen, A. Santana, A. McCaskey, R. Herrman, J. Ostrowski, G. Siopsis, and T. S. Humble, "Scaling quantum approximate optimization on near-term hardware," *Scientific Reports*, vol. 12, no. 1, p. 12388, 2022.
- [3] M. Bostock, V. Ogievetsky, and J. Heer, "D³ data-driven documents." *IEEE Transactions on Visualization and Computer Graphics*, vol. 17, no. 12, pp. 2301–2309, 2011.
- [4] S. Dasgupta. (2023) Quantum characterization metrics data set. [Online]. Available: <https://github.com/quantumcomputing-lab/nisqReliability/>
- [5] B. Shneiderman, "The eyes have it: A task by data type taxonomy for information visualizations," in *IEEE Symposium on Visual Languages*, Sep 1996, pp. 336–343.
- [6] A. Inselberg, "The plane with parallel coordinates," *The Visual Computer*, vol. 1, no. 2, pp. 69–91, 1985.
- [7] C. A. Steed, J. R. Goodall, J. Chae, and A. Trofimov, "Crossvis: A visual analytics system for exploring heterogeneous multivariate data with applications to materials and climate sciences," *Graphics & Visual Computing*, vol. 3, p. 200013, 2020.
- [8] R. Tavenard, J. Faouzi, G. Vandewiele, F. Divo, G. Androz, C. Holtz, M. Payne, R. Yurchak, M. Rußwurm, K. Kolar, and E. Woods, "Tsklearn, a machine learning toolkit for time series data," *Journal of Machine Learning Research*, vol. 21, no. 118, pp. 1–6, 2020. [Online]. Available: <http://jmlr.org/papers/v21/20-091.html>
- [9] F. Petitjean, A. Ketterlin, and P. Gançarski, "A global averaging method for dynamic time warping, with applications to clustering," *Pattern recognition*, vol. 44, no. 3, pp. 678–693, 2011.